Use of Water and Mercury Droplets to Simulate Al_2O_3 Collision/Coalescence in Rocket Motors

Mark Salita*
Thiokol Corporation, Brigham City, Utah 84302

Combustion of aluminized solid propellants produces aluminum oxide droplets in a wide range of sizes. Droplets of different sizes accelerate at different rates and may collide, especially in nozzles of rocket motors. It has generally been assumed in the past that all collisions among these droplets result in coalescence. However, a model for coalescence efficiency previously developed and verified experimentally for free-falling water droplets indicates that permanent coalescence will not occur if the rotational energy of the spinning (temporarily coalesced) agglomerate exceeds the surface energy holding it together. Consequently, the extrapolation of this model to the high surface tension and impact energies of Al_2O_3 droplets in nozzles has been studied experimentally using mercury droplets because 1) their liquidity at room temperature allows for simple and inexpensive testing, 2) they have a surface tension that is nearly that of Al_2O_3, 3) their large diameters are easily visible, and 4) their high density generates high-impact energy at low-impact velocity. Single mercury droplets (bullets) of various diameters were rolled into a stationary mercury droplet (target) and the collision/coalescence process was recorded on videotape; bullet size, speed, and offset were obtained from a superposed grid. It was concluded that the water model accurately predicts the collision-induced coalescence of mercury and, therefore, Al_2O_3 droplets because 1) the qualitative similarity between the collision/coalescence behavior of water droplets and liquid metal (mercury) droplets was excellent, 2) the model predicts well quantitatively whether a collision will result in coalesced mercury droplets, and 3) the model predicts well the degree of Al_2O_3 coalescence apparently occurring in the nozzle of the Space Shuttle booster.

Nomenclature

E_R = rotational energy of spinning agglomerate
E_s = surface energy of agglomerate
E_T = energy required to tear agglomerate apart
F, G, H = efficiency dependence on Z
g = gravitational acceleration
h = drop height of mercury bullet
I = moment of inertia of agglomerate
M = mass of target
m = mass of bullet
N = number of product drops formed during noncoalescence
R = radius of spherical target
R_o = radius of coalesced spherical agglomerate
r = radius of spherical bullet
r_i' = radius of ith product droplet
U = impact velocity of bullet with target
W = droplet Weber number, $\rho U^2 r/\sigma$
x = collision offset relative to center of target mass
x_{cr} = critical collision offset above which noncoalescence occurs
Z = diameter ratio of bullet to target
η = coalescence efficiency
ρ = mass density of all droplets
σ = surface tension of droplet
$\Omega, \bar{\Omega}$ = dimensional and normalized angular momentum of coalesced agglomerate, respectively
ω = angular velocity of coalesced agglomerate

Introduction

COMBUSTION of aluminized solid propellants produces a mixture of gas and Al_2O_3 droplets. The droplet size distribution in the combustion chamber is typically bimodal and polydisperse; the distribution of mass in each mode is approximately log normal with diameter, and the mass-mean diameter of each mode is roughly 1 and 100 μm, respectively.[1] Acceleration of the gas/particle mixture in the rocket motor (especially in the nozzle) causes the diameter of all droplets to change: 1) all droplets shrink due to solidification and density increase as they cool, and 2) the large droplets suffer aerodynamic breakup and collision/coalescence caused by velocity differences between the gas and large droplets and among droplets of different sizes. The effect of collision/coalescence depends on the frequency of collisions of larger/slower droplets with smaller/faster droplets and on the chance that these collisions result in coalescence.

All of these size-change mechanisms, except coalescence, have previously been studied and modeled, for example, during development of the Air Force Rocket Propulsion Laboratory (AFRPL) sponsored one-dimensional three phase (OD3P) nozzle flow code.[2] In particular, models for collision efficiency as a function of droplet Reynolds and Stokes numbers have been developed, but it has usually been assumed that all collisions result in coalescence due to the absence of a model for metal droplet coalescence. Unfortunately, a more recent study of collision/coalescence[4] showed that coalescence efficiency can have a very large effect on particle size. When applied to the redesigned Space Shuttle booster (RSRM), the industry-standard assumption of 100% coalescence predicts a monomodal mass-mean Al_2O_3 particle diameter at the nozzle exit that is twice that predicted by Hermsen's industry-standard correlation,[5] whereas, the assumption of 0% coalescence predicts half the correlated size and a bimodal size distribution. An accurate model for coalescence efficiency is thus required to predict particle size distributions in solid-propellant rocket motors and their plumes.

Consequently, a study of droplet coalescence was undertaken. The term collision/coalescence is used here to describe the coalescence behavior that results from a collision of specified energy and offset. An existing model for water droplet coalescence[3] was available that had been shown to match water droplet measurements and has been applied successfully in numerous liquid-fuel atomization studies. The model assumes that all liquid droplet collisions result in at least tem-

Received Oct. 30, 1989; revision received July 25, 1990; accepted for publication July 26, 1990.
*Senior Scientist. Member AIAA.

porary coalescence, with the coalescence remaining stable (permanent) only if the rotational energy of the spinning agglomerate does not exceed the surface energy required to hold it together; if the coalescence is unstable, the agglomerate is assumed to break into two spherical droplets with the same masses as the original colliding spherical droplets. The model depends only on the droplet Weber number W and the ratio of diameters Z of the colliding droplets.

Three steps were taken to determine whether this model could also be applied accurately to Al_2O_3 and other liquid-metal oxide droplets (whose surface tension is as much as 10 times that of water and liquid fuel):

1) The model was rederived for arbitrary size and number of product droplets.

2) A series of collision/coalescence experiments was conducted at room temperature using mercury droplets, whose high surface tension is nearly that of Al_2O_3 and whose high density allowed low-velocity collisions to simulate the impact energy of Al_2O_3 collisions in a motor.

3) The model was implemented in OD3P to predict the mean diameter of Al_2O_3 particles at the exit of the RSRM; improved agreement with Hermsen's correlation would improve confidence in the extrapolation of the water/mercury model to Al_2O_3.

Modeling of Water Droplet Coalescence

Brazier-Smith et al.[3] measured and modeled the coalescence of water droplets colliding in air. They postulated that when two droplets collide they will always coalesce at least temporarily (except for the infrequent case of grazing collisions), but they will break apart if the rotational energy of the resulting agglomerate exceeds the surface energy holding it together, with the final separated droplets being identical to the incident droplets (Figs. 1). They were able to show excellent agreement between the coalescence efficiency predicted by this model and that measured in a series of water droplet experiments (Figs. 2). Their model is now summarized and rederived allowing for arbitrary number and size of product droplets.

Suppose a smaller spherical droplet of radius r and mass m approaches a larger spherical droplet of radius R and mass M with a relative velocity U along a line offset by a distance x from the center of the larger dropet (Fig. 1a). Assume that upon impact the smaller droplet (bullet) coalesces at least temporarily with the larger (target) droplet to form an agglomerate sphere of mass $m + M$ and radius $R_o = (R^3 + r^3)^{1/3}$. The center of mass of the agglomerate lies a distance x_c from the trajectory of the bullet and is given by

$$m \cdot o + Mx = (m + M)x_c \rightarrow x_c = \frac{xR^3}{R_o^3} \tag{1}$$

Assuming that the mass density of the colliding and agglomerated droplets are the same, then the impact imparts an angular momentum Ω to the agglomerate (Fig. 1b) given by

$$\Omega = mUx_c = \frac{4}{3}\pi\rho U\frac{xR^3r^3}{R_o^3} \tag{2}$$

which immediately spins about the center of mass with angular velocity ω given by

$$\omega = \frac{\Omega}{I} \tag{3}$$

where I is the moment of inertia of the agglomerate sphere

$$I = \frac{2}{5}(m + M)R_o^3 \tag{4}$$

The resulting rotational energy of the spinning agglomerate is

$$E_R = \frac{1}{2}I\omega^2 = \frac{\Omega^2}{2I} = \frac{5\pi}{3}\rho U^2\frac{x^2R^6r^6}{R_o^{11}} \tag{5}$$

If this rotational energy is large enough, the surface energy holding the agglomerate together will be overcome and it will shatter into N multiple product droplets of radii r_i' (Fig. 1c). Since the surface energy of the agglomerate droplet is

$$E_s = 4\pi\sigma R_o^2 \tag{6}$$

then the energy required to tear the agglomerate into the N component droplets is

$$E_T = 4\pi\sigma\left[\sum_{i=1}^{N}(r_i')^2 - R_o^2\right] \tag{7}$$

where conservation of mass requires

$$\sum_{i}^{N}(r_i')^3 = R_o^3$$

Thus, the condition for noncoalescence of the bullet and target

$$E_R > E_T \tag{8}$$

becomes

$$x^2 > \frac{12}{5}\frac{\sigma}{\rho U^2 r}\frac{R_o^{11}}{R^6r^5}\left[\sum_{i=1}^{N}(r_i')^2 - R_o^2\right] \tag{9}$$

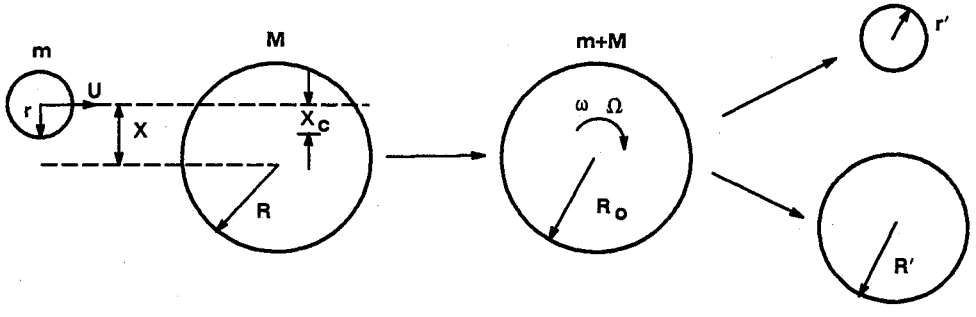

a) Collision b) Coalescence c) Noncoalescence (rotational energy > surface energy).

Fig. 1 Coalescence and noncoalescence of colliding droplets.

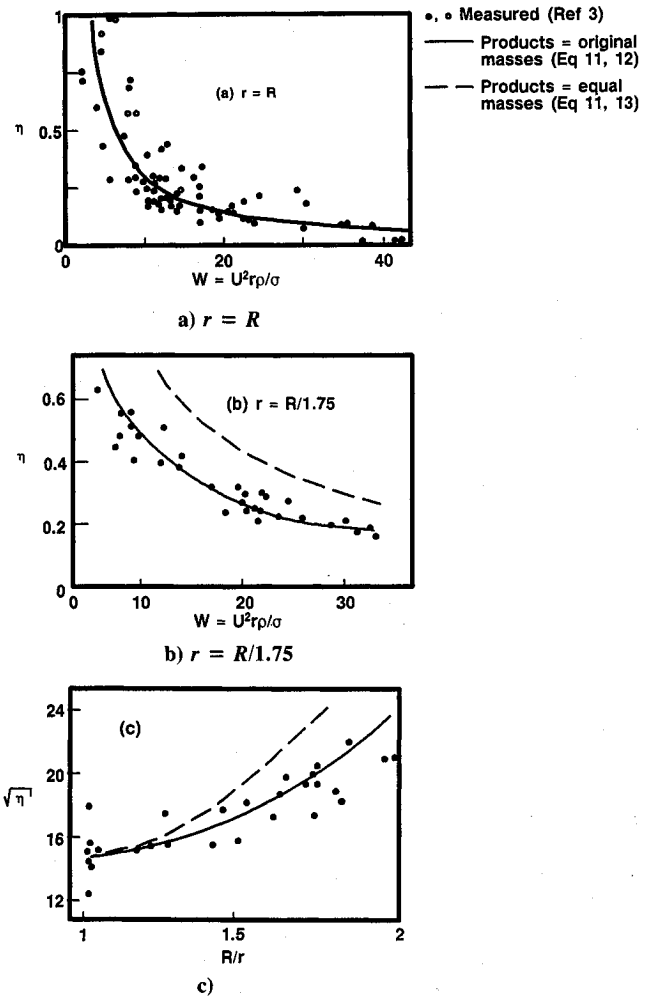

Fig. 2 Coalescence efficiency for water droplets.

The coalescence efficiency η is the ratio of the collision cross section that results in coalescence (πx^2) to the maximum possible collision cross section [$\pi(R + r)^2$]:

$$\eta = \frac{x_{cr}^2}{(R + r)^2} \tag{10}$$

Hence, Eqs. 9 and 10 yield

$$\eta = \frac{12/5}{W} F(Z, G) \tag{11}$$

where

$W = \rho U^2 r/\sigma$ is the droplet Weber number

$$F = \frac{(1 + Z^3)^{11/3}}{Z^5(1 + Z)^2}[G - (1 + Z^3)^{2/3}]$$

$$G = \sum_i^N (r_i'/R)^2$$

$$Z = \frac{r}{R}$$

This solution obviously depends on the nature of the shattered agglomerate (i.e., G). Although many scenarios can be imagined, two asymptotic cases are studied here. If only two product droplets are generated and they are the same size as the bullet and target (as assumed in Ref. 3), then

$$G = 1 + Z^2 \tag{12}$$

If, on the other hand, the two product droplets are of equal size, then

$$G = 2^{1/3}(1 + Z^3)^{2/3} \tag{13}$$

Note that Eqs. (12) and (13) are identical ($G = 2$) only when bullet and target are the same size ($Z = 1$).

The measured coalescence efficiency reported in Ref. 3 for colliding water droplets is compared in Figs. 2 to that predicted by Eq. (11) for both product-droplet assumptions; good agreement is achieved only if the two product droplets are the same size as the bullet and target. The failure of the equal-mass, product-droplet scenario [Eq. (13)] explains why the momentum-criterion approach, also presented in Ref. 3, was unsuccessful. Defining a normalized angular momentum $\bar{\Omega}$ by

$$\bar{\Omega}^2 = \frac{\Omega^2}{\sigma\rho R_o^7} = \frac{16\pi^2}{9} W \frac{x^2}{R^2} \frac{Z^5}{(1 + Z^3)^{13/3}} \tag{14}$$

then Eq. 10 becomes

$$\eta = \frac{12/5}{W} \bar{\Omega}_{cr}^2 H(Z) \tag{15}$$

where

$$H = \frac{15}{64\pi^2} \frac{(1 + Z^3)^{13/3}}{Z^5(1 + Z)^2}$$

Equivalence of the momentum and energy criteria [Eqs. (11) and (15)] yields the condition on the critical angular momentum for noncoalescence:

$$\bar{\Omega}_{cr} = 8\pi \sqrt{\frac{G/(1 + Z^3)^{2/3} - 1}{15}} \tag{16}$$

Thus, the assumption in Ref. 3 that $\bar{\Omega}_{cr}$ is a universal constant (12.62 for cusping instability, 5.0 for toroidal instability) is seen to be invalid unless the product droplets are of equal mass, whence use of Eqs. (13) and (16) yield $\bar{\Omega}_{cr} = 3.31$. However, successful simulation of the water data required product droplets equal in size to bullet and target, which implies that $\bar{\Omega}_{cr}$ depends strongly on Z; indeed, choices for Z of 0.1, 0.5, and 1.0 yield $\bar{\Omega}_{cr} = 0.63$, 2.56, and 3.31, respectively.

These results support for water the postulation of Ref. 3 that unstable coalesced droplets will separate into the original bullet and target masses. However, it was deemed possible that droplets of high surface tension (the surface tension of Al_2O_3 is as much as 10 times that of water) could lose their memory during temporary collision/coalescence. Consequently, collision/coalescence experiments were conducted using mercury droplets (whose surface tension at room temperature is comparable to that of liquid Al_2O_3).

Mercury Droplet Experiments

Since Al_2O_3 is liquid only above 2327°K, direct measurement of Al_2O_3 droplet coalescence would require expensive hot motor firings for which no diagnostic techniques are available. If experiments could be conducted at room temperature, cost could be minimized and measurement/visualization techniques would be available. Mercury is the only common high-surface-tension material that is liquid at room temperature, and its high density allows high-impact energies to be generated with relatively small-impact velocities (Table 1). Indeed, sufficiently large impact velocities can be achieved easily in the laboratory using mercury droplets to simulate collisions of Al_2O_3 droplets in a rocket nozzle. This can be shown by noting that Eq. (11) requires only that the droplet Weber

Table 1 Material properties of water, aluminum oxide, and mercury

Property	Water	Mercury	Al_2O_3(liquid)
Density ρ, gm/cc	1.0	13.52	2.40
Surface tension σ, dynes/cm	75	485	600
Typical droplet diameters, μ			
Small	150	1500	1
Large	750	3175[a]	100

[a] $\frac{1}{8}$ in.

Fig. 3 Ski slope apparatus for mercury droplet experiments.

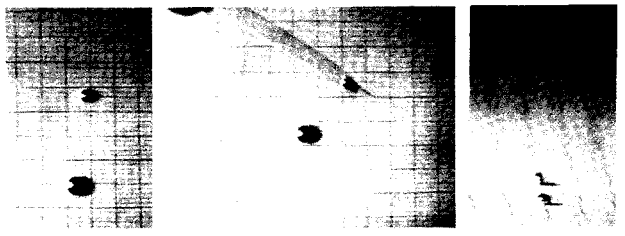

Fig. 4 Test preparation: a) sizing bullet and target; b) moving bullet to drop point with dropper; c) horizontal view of bullet roll just prior to collision with target.

number W and radius ratio Z be the same in both environments. Since a maximum impact velocity of 183 m/s (600 ft/s) is predicted by OD3P for 1-μm Al_2O_3 bullets in the RSRM nozzle,[4] then W similitude requires that mercury droplets of diameter 0.3 cm ($\frac{1}{8}$ in.) must impact with a maximum velocity of only

$$U_{Hg} = \alpha U_{Al_2O_3} = 1.2 \text{ m/s } (4.0 \text{ ft/s})$$

since

$$\alpha = \sqrt{\frac{(\rho r/\sigma)_{Al_2O_3}}{(\rho r/\sigma)_{Hg}}} = 0.0067$$

Since these velocities are generated easily in the laboratory, a series of simple collision/coalescence experiments were conducted using mercury droplets.

Ideal simulation of Al_2O_3 collision/coalescence in a rocket motor would require mercury droplets to be fired through the air at each other. However, the cost of the control apparatus to accomplish this was prohibitive, and so mercury droplets (bullets) were rolled down an inclined surface (ski slope) such as to collide with stationary mercury droplet targets at the bottom of the slope (Fig. 3). Use of plastic or teflon surfaces caused material shedding from the droplet during its roll, but covering the surface with graph paper eliminated this problem (by reducing wetting) and provided a means of determining droplet sizes and velocities (Figs. 4). The collision/coalescence event was recorded using a high-speed (60 frames/s), fast-shutter (1 ms) video camera. Attempts to record the event using an open-shutter still camera in a dark room with high-frequency strobe light failed due to inadequate strobe intensity and image size.

Target diameters were identified easily from their stationary position on the graph paper; typical diameters were 0.36 cm (0.14 in.) (2 axial lines). Bullet diameters could not be identified during the test due to their distortion during roll; consequently, they were determined before the test by temporary stationary placement on the graph paper (Fig. 4a).

Bullet velocities were determined by counting the number of graph-paper lines traversed by the droplet in one frame (1/60 s) in tests conducted without targets; impact velocities were deduced to be 85.3, 106.7, and 117.3 cm/s (2.80, 3.50, and 3.85 ft/s) for both large and small bullets for vertical drops h of 5, 10, and 15 cm (2, 4, and 6 in.), respectively. These measured velocities agree within 20% with those estimated from an energy balance for a rolling disk:

$$mgh = \frac{1}{2} mU_o^2 + \frac{1}{2} I\omega_o^2 \tag{17}$$

where

$$I = \frac{mr^2}{2}, \qquad \omega_o = \frac{U_o}{r}$$

so that

$$U_o = \sqrt{4gh/3}$$

$$= 81.4, 115.2, 141.1 \text{ cm/s } (2.67, 3.78, 4.63 \text{ ft/s})$$

Knowledge of this impact velocity and the measured bullet and target diameters allowed determination of the droplet Weber number; the critical offset for the test could then be estimated from Eqs. (10) and (11). Inaccuracy in this prediction arose primarily from two sources: 1) imprecision in determining collision offset from the video frames, and 2) nonsimilitudes introduced by the droplet/surface interaction. The resolution of the collision offset was about one-quarter of a graphical box, i.e., about 10% of the target diameter. The principal nonsimilitudes introduced by the surface were the following:

1) The rolling bullets were spinning, thereby causing the initially spherical bullet to deform into a disk (wheel-like) shape, which (probably unlike Al_2O_3 droplets) struck the target with a component of tangential as well as axial impact velocity.

2) The targets were slightly flattened by gravity into a somewhat nonspherical shape.

3) Spin velocities of the targets after collision were reduced slightly by surface friction, thereby slightly increasing the chance of coalescence.

In spite of these nonsimilitudes between the model and the experiments, it was felt that the critical collision offset could be predicted within $\pm 10\%$ because of the following:

1) The shape of the bullet has little effect since only its mass and offset are needed in Eqs. (1) and (2).

2) The precollision distortion of the target was negligible compared to the nonspherical nature of the agglomerate immediately after collision; however, nonspherical agglomerate shape occurred in the water droplet experiments without invalidating the simplified model (Fig. 2).

3) Surface friction is relatively unimportant due to the high surface tension of mercury and the absence of wetting of the mercury on the graph paper.

Three series of tests were conducted (Table 2) to study the effect of impact velocity U, bullet/target size ratio Z, and collision offset x. Typical results are shown in Figs. 5–11 in the form of sequences of video frames taken 1/60 s apart during the collision event. (It should be noted that the original video record provides far better clarity for discerning droplet sizes and offset.) Figure 5 shows that even at high-impact velocity, a small bullet without offset can result in coalescence.

Table 2 Results of mercury droplet experiments[a]

		Test Results						Predictions[b]		
Series	Type	Test number	H, in.	Z	X/R	Coalescence	Satellites	W	X_{cr}/R	Coalescence
1	Half bullet	12	2	1/2	0	Yes	—	18	1.05	Yes
		11	2	1/2	0	Yes	—	18	1.05	Yes
	(No offset)	10	4	1/2	0	Yes	—	28	0.84	Yes
		9	4	1/2	0	Yes	—	28	0.84	Yes
		15	6	1/2	0	Yes	—	34	0.77	Yes
2	Full bullet	4	2	1	0	Yes	—	36	0.59	Yes
		3	2	1	0	Yes	—	36	0.59	Yes
	(No offset)	2	4	1	0	Yes	—	56	0.47	Yes
		1	4	1	0	Yes	—	56	0.47	Yes
		5b	4	1	0	Yes	—	56	0.47	Yes
3	Offset	5a	4	2/3	0.21	Yes	—	38	0.56	Yes
		5a′	4	1/2	0.43	Yes	—	28	0.84	Yes
		6	4	1	0.43	No	1	56	0.47	Yes[c]
		5c	4	1	0.43	No	0	56	0.47	Yes[c]
		13	6	1	0.43	No	0	68	0.43	No[c]
		14	6	1	0.49	No	1	68	0.43	No
		8	2	1	0.64	Yes	—	36	0.59	No[c]
		7	2	1	0.43	Yes	—	36	0.59	Yes
		5	4	1	0.86	No	4	56	0.47	No
		24	8	1/2	1.00	No	3	72	0.53	No
		25	8	1/2	0.69	No	1	90	0.47	No
		26	6	1/2	0.86	No	5	42	0.69	No
		27	6	1/2	0.86	No	0	42	0.69	No
		28	6	1/2	0.69	No	1	42	0.69	No[c]
		29	6	1/2	0.86	No	3	51	0.63	No
		30	6	1/2	0.64	No	5	68	0.54	No

[a]Tests 16–23 were used to determine impact velocities in the absence of targets.
[b]Noncoalescence is predicted to occur if $X > X_{cr}$ (assuming product droplets have original sizes).
[c]Within ±10% experimental uncertainty.

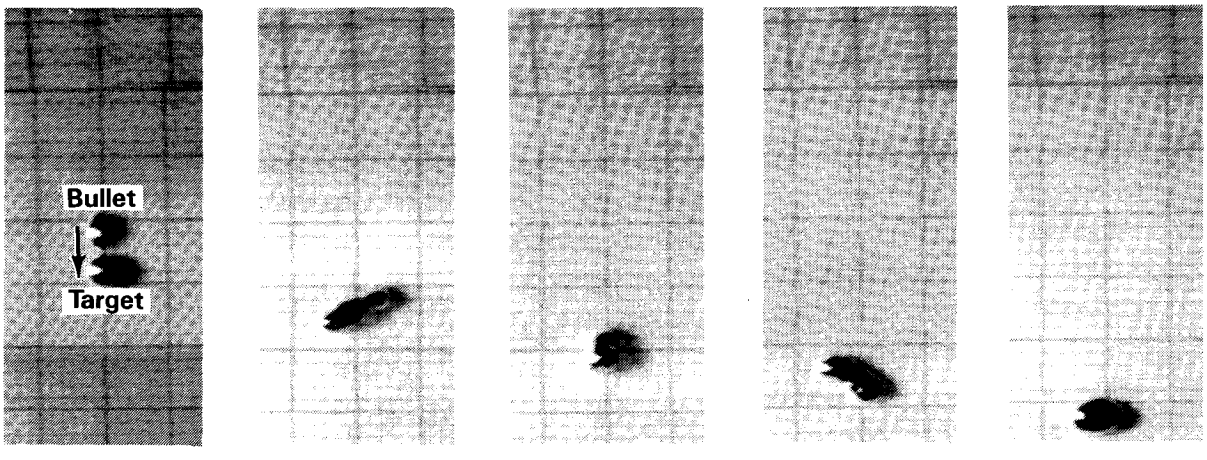

Fig. 5 Mercury droplet test 15: fast, half-size bullet without offset.

Figure 6 shows that even a large bullet at moderate-impact velocity without offset can result in coalescence. Figure 7 shows that even a large bullet at large offset can result in coalescence if it is moving slowly enough. Figure 8 shows that high-impact velocity can lead to noncoalescence if the bullet and offset are large enough; two product droplets are formed that appear equal in size to each other and the original bullet and target. Figure 9 shows that a large bullet at large offset can result in noncoalescence even for moderate impact velocities; despite the formation of multiple satellite droplets (analogous to the water droplet experiment shown in Fig. 11), two product droplets comprise almost the entire mass. Figure 10 shows that even small bullets can result in noncoalescence if the offset and impact velocity are large enough; the two product droplets are essentially the original bullet and target with the five satellite droplets comprising very little mass. Figure 11 shows that the noncoalescence behavior of mercury droplets looks very similar qualitatively to that of water droplets.

Table 2 shows that Eqs. (11) and (12) provide an accurate technique for predicting whether collision will end in coalescence in spite of 1) the nonsimilitudes between the model assumptions and the test conditions (nonspherical spinning droplets, surface friction), and 2) the approximate method of estimating droplet velocities, sizes, and offsets from the video frames. All 10 tests without collision offset were predicted correctly to result in coalescence regardless of impact velocity or size ratio. In 13 of the 16 tests with offset, the coalescence behavior was predicted correctly by Eqs. (11) and (12); indeed, all 3 tests incorrectly predicted (as well as 2 correctly predicted) were within the experimental uncertainty of the tests (x within ±10% of x_{cr}).

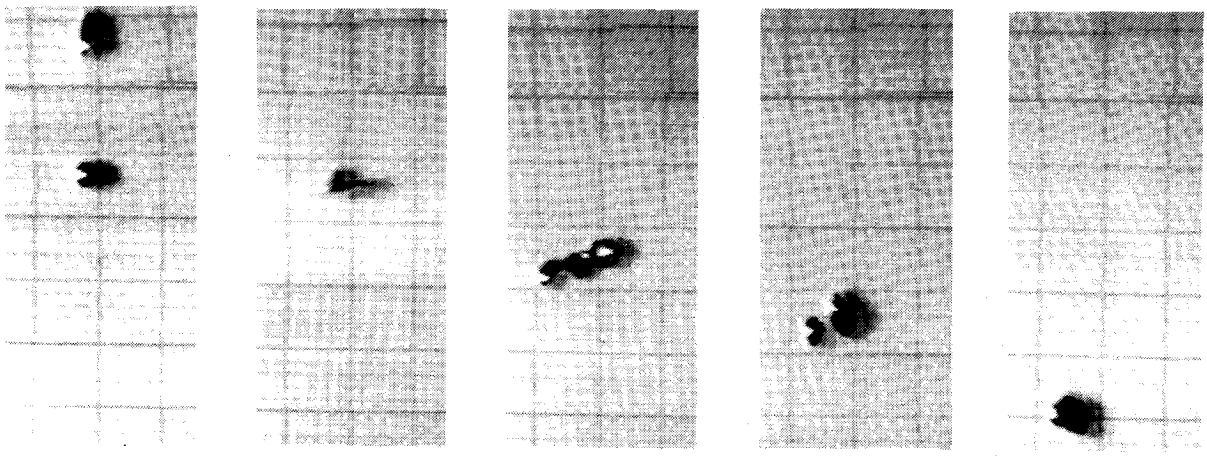

Fig. 6 Mercury droplet test 5b: moderate-speed, full-size bullet without offset.

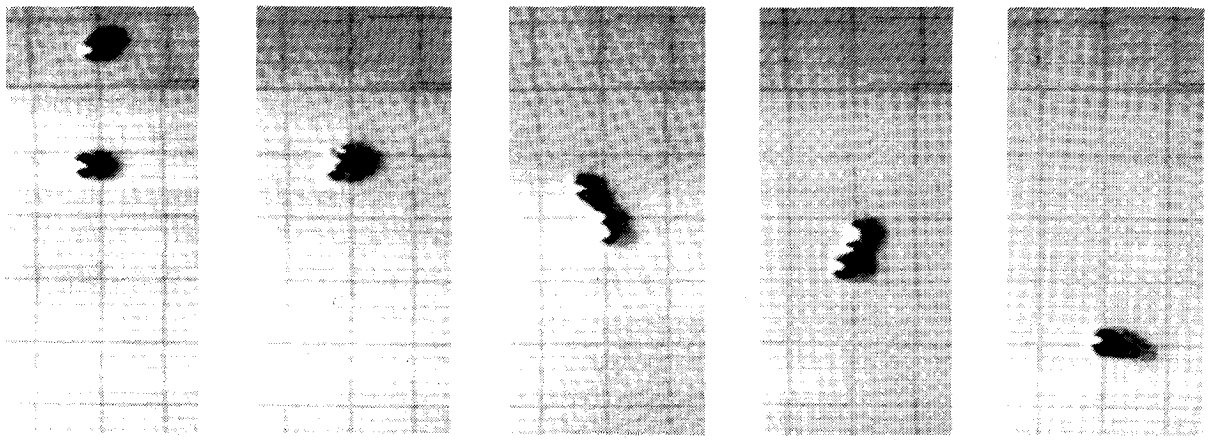

Fig. 7 Mercury droplet test 7: slow, full-size bullet with half offset.

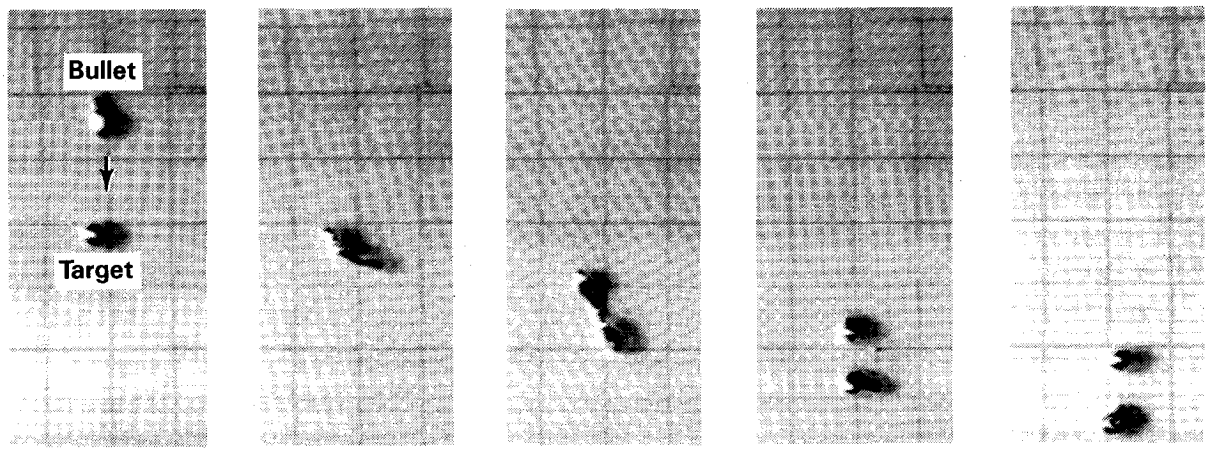

Fig. 8 Mercury droplet test 14: fast, full-size bullet with half offset.

Application to Solid Rocket Motor

The collision/coalescence of Al_2O_3 droplets in the nozzle of a solid rocket motor depends strongly on the distribution of droplet sizes entering the nozzle inlet. Quench-bomb measurements[1] of the particulate generated by a range of aluminized propellants have shown that the droplet size distribution in the motor combustion chamber is bimodal log normal with 1) about $\frac{2}{3}$ of the droplet mass comprised of small (smoke) particles whose mass-mean diameter is about 1.5 μ and whose standard deviation is about 0.4, and 2) about $\frac{1}{3}$ of the droplet mass comprised of large particles whose mass-mean diameter varies with motor pressure and propellant from about 40 to 700 μ but whose standard deviation is usually about 0.2. Although the large particles are quickly broken down by the lag-induced shear forces in the nozzle, there is still a large difference in size and, therefore, velocity between the two particle modes; this causes a high-collision frequency at high-impact energies.

Figure 12 shows the variation of mean particle diameter D_{43} throughout the nozzle of the RSRM as predicted by OD3P with the continuous size distribution approximated by 10 dis-

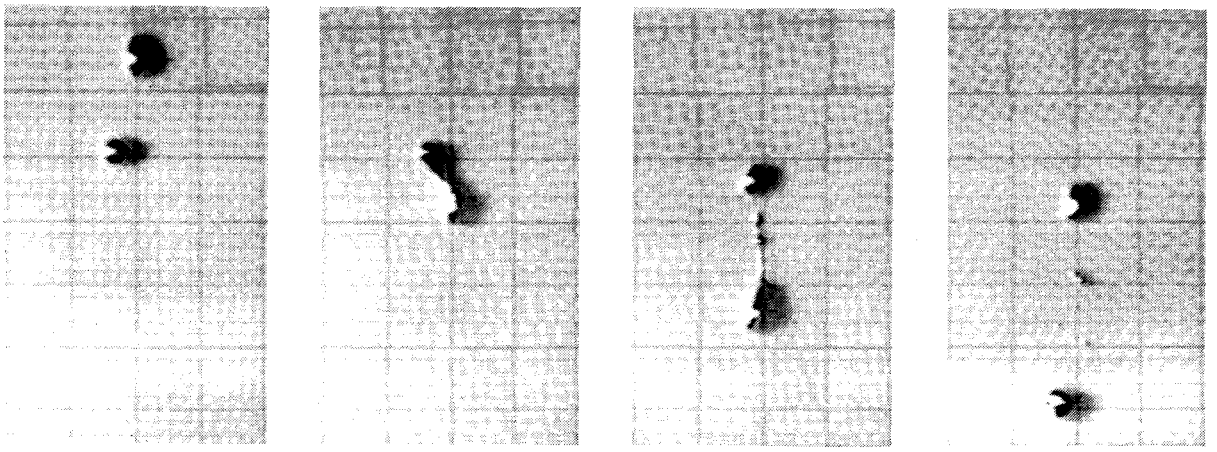

Fig. 9 Mercury droplet test 5: moderate-speed, full-size bullet with full offset.

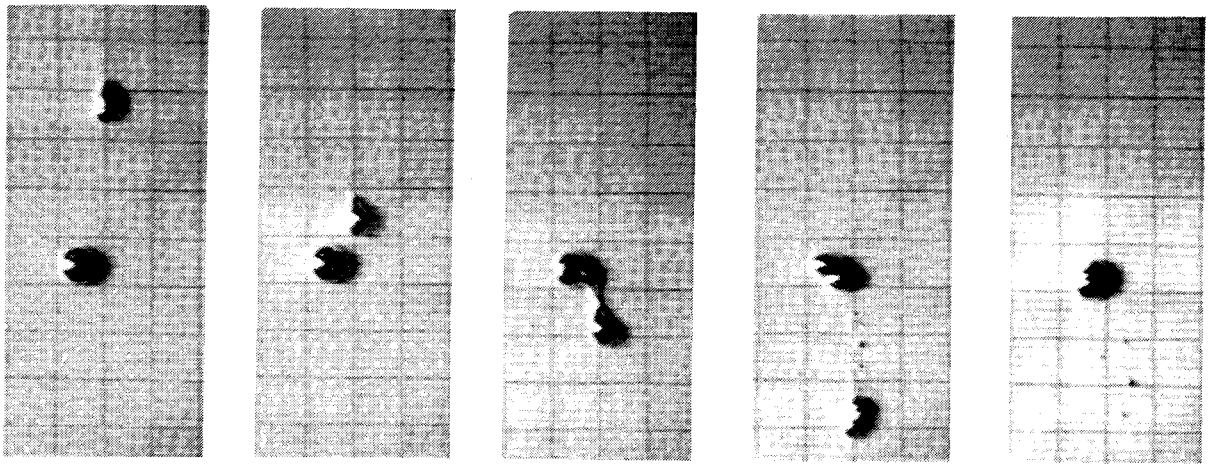

Fig. 10 Mercury droplet test 30: fast, half-size bullet with extreme offset.

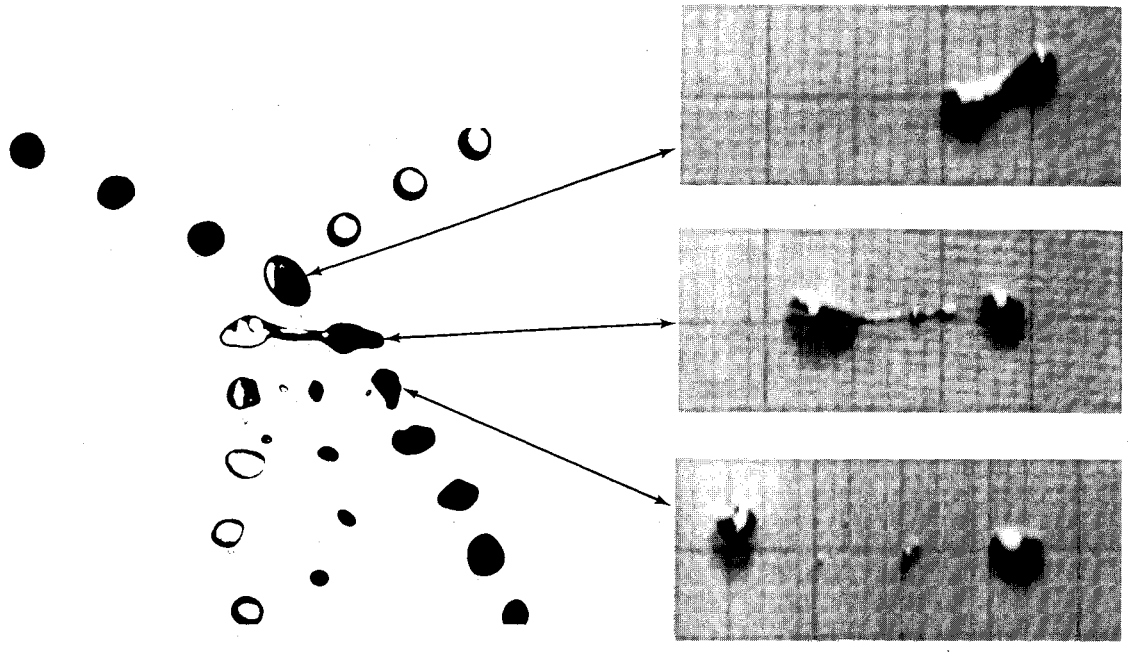

Fig. 11 Similarity of noncoalescence behavior of water and mercury droplets.

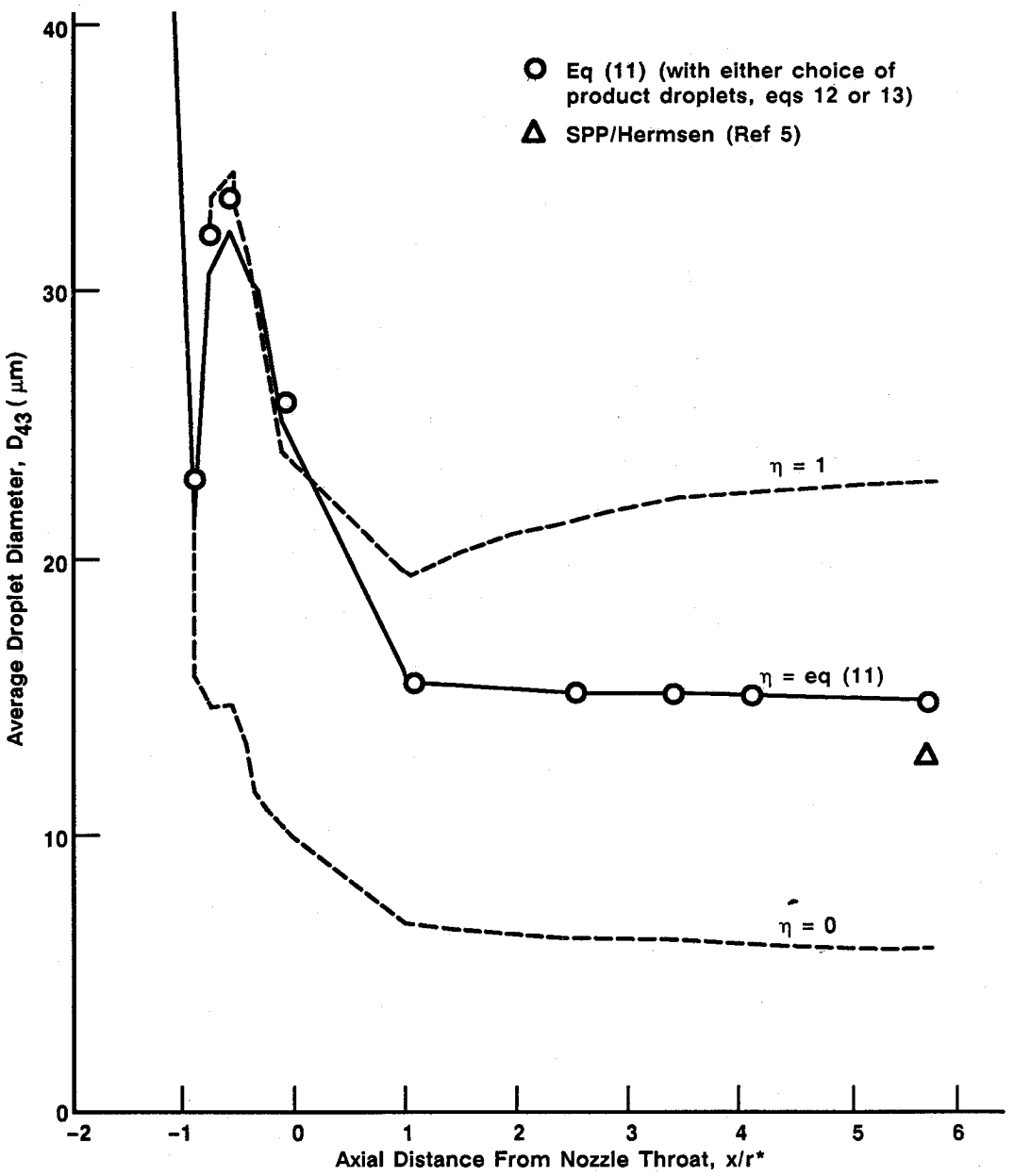

Fig. 12 Effect of coalescence efficiency on D43 as predicted by OD3P code for RSRM.

crete diameters. It is seen that the assumption of 100% coalescence efficiency generates a D_{43} at the nozzle exit that is about twice that predicted by Hermsen's industry-standard correlation, whereas the assumption of 0% coalescence efficiency generates a D_{43} that is half the value predicted by the correlation. Use of Eq. (11) results in an intermediate coalescence efficiency that predicts an exit D_{43} within 15% of the correlation; this was caused by nearly complete coalescence during collisions of smoke and large particles but only 5% coalescence during collisions among the large particles. Since the correlation is only accurate to within about 20%, it is concluded that Eq. (11) predicts well the coalescence of Al_2O_3 droplets in solid rocket nozzles.

Finally, it should be noted that the nearly complete coalescence of smoke with large particles results in a monomodal mass-weighted size distribution at the nozzle exit. However, the 0.2% of mass that remains as smoke causes the number density of smoke particles still to be twice that of the large particles since the exit diameter of a smoke particle is roughly one-tenth that of a large particle. This is a significant result for the plume analyst since the emissive behavior of plumes is dependent on the square of the number density of the particles.

Acknowledgments

The author is indebted to Mike Harper, whose ingenuity allowed the concept of mercury droplet experimentation to be successfully implemented, and to Robert Goodell and Greg Price, whose expertise at conducting the experiments led to a clear and enlightening video record as well as results that were consistent, repeatable, and quantifiable.

References

[1]Salita, M., "Quench Bomb Investigation of Al_2O_3 Formation from Solid Rocket Propellants Part II: Analysis of Data," CPIA 498 (Vol. I), *25th JANNAF Combustion Meeting*, Oct. 1988, pp. 185–197.

[2]Hunter, S. C., et al., "One-Dimensional Three-Phase Reacting Flow with Mass Transfer Between Phases," Air Force Rocket Propulsion Laboratory TR-81-103, Sept. 1986.

[3]Brazier-Smith, P. R., Jennings, S. G., and Latham, J., "The Interaction of Falling Water Drops: Coalescence," *Proceedings of the Royal Society of London, Series A*, Vol. 326, 1972, pp. 393–408.

[4]Salita, M., "Implementation and Validation of the One-Dimensional Gas/Particle Nozzle Flow Code OD3P," CPIA 529 (Vol. II), *26th JANNAF Combustion Meeting*, Oct. 1989, pp. 69–82.

[5]Hermsen, R. W., "Aluminum Oxide Particle Size for Solid Rocket Motor Performance Prediction," *Journal of Spacecraft and Rockets*, Vol. 18, No. 6, 1981, pp. 483–490.